# The novel MuRF2 target SNX5 regulates PKA activity through stabilization of RI-α and controls myogenic differentiation

Ning Li[1,2], Jida Hamati[3], Yi Li[1,3], Björn Brinschwitz[1,2], Mohamed Ghait[1,2], Elisa Martin[1,2], Dörte Lodka[3], Elke Hammer[1,4], Britta Fielitz[1,2], Uwe Völker[1,4], Gunnar Dittmar[5,6], Thomas Sommer[7,8,9], Friedrich C. Luft[3], Jens Fielitz[1,2,3*]

## Supplementary Methods

### Cell culture experiments

COS-7 cells (ATCC, CRL-1651) and HEK293 cells (ATCC, USA; CRL-1573) were cultured in Dulbecco's Modified Eagle Medium (DMEM, 4.5g/L glucose, Gibco™, Thermo Fisher Scientific, USA) supplemented with 10% fetal bovine serum (FBS), 2 mM glutamine, 1 U/ml penicillin, and 1 µg/ml streptomycin (all from Sigma-Aldrich, Germany) at 37°C in a 5% $CO_2$ atmosphere. C2C12 cells (ATCC, USA, CRL-1772) were cultivated in growth medium (GM; DMEM, 1g/l glucose, PAN-Biotech, Germany) supplemented with 10% FBS, 2 mM glutamine, 1 U/ml penicillin, and 1 µg/ml streptomycin (all from Sigma-Aldrich, Germany). For differentiation, C2C12 myoblasts at 80% confluency were transferred to differentiation medium (DM; DMEM, 1g/L glucose, 2% FBS, 2 mM glutamine, 1 U/ml penicillin, and 1 µg/ml streptomycin (all from Sigma-Aldrich, Germany) for indicated time points with daily medium exchange. Following chemicals were used to treat cells: cycloheximide (100 µg/ml, CHX), chloroquine (50 µM, CQ), dibutyryl cyclic adenosine monophosphate (1 mM, Bt2cAMP) (all Sigma-Aldrich, Germany), MG132 (C2C12: 10 µM, COS-7: 25 µM, Merck, Germany), bafilomycin A1 (200 nM, BafA1, Cell Signaling, USA), phorbol 12-myristate 13-acetate (100 nM, PMA, InvivoGen, USA), recombinant myostatin (100 ng/ml, MSTN, Proteintech, UK), reconstitution buffer (4 mM HCl, 0.1% BSA).

### Generation of cDNA expression plasmids and site directed mutagenesis

The coding sequences of *Trim55* (MuRF2), *Trim54* (MuRF3) and *Snx5* (SNX5) were amplified from mouse muscle cDNA by PCR using primer pairs containing restriction enzyme consensus sequences (primer sequences are shown in Table S1). cDNA expression plasmids were used as a template with specific primer pairs (shown in Table S4) to synthesize deletion mutants. To generate E3 ligase deficient *Trim55* and *Trim63* cDNA expression plasmids cysteine residues Cys42 and Cys50 in MuRF2 and MuRF3 RING-finger domains were mutated

into serine residues using the Phusion™ site-directed mutagenesis kit (Thermo Fisher Scientific, USA). Primers were designed according to the manufacturer's protocol (Table S4). SNX5 lysine-to-arginine mutants were generated by using the QuikChange II site-directed mutagenesis kit (Agilent Technologies, USA) with primers that were designed according to the manufacturer's protocol (Table S4). cDNA expression plasmids were sequence verified.

**Transfection**

COS-7 and HEK293 cells were transfected using FuGENE-6 (Roche, Switzerland) according to the manufacturer's recommendations. Lipofectamine and PLUS™ reagent (both Invitrogen, USA) were used to transfect cDNA expression plasmids into C2C12 cells according to the manufacturer's protocol. For siRNA transfection, non-target (NT)-siRNA (D-001810-10-05) and SNX5-siRNA (J-060939-09-1101) were transfected into C2C12 cells with Dharmafect3 (all from Dharmacon, USA) according to the manufacturer's protocol.

**Retrovirus production and transduction of C2C12 cells**

The coding sequence of *Snx5* were PCR amplified (Primers are shown in Table S5) and subcloned into a retroviral expression plasmid (pMP71-IRES-GFP). Plat-E cells (Platinum-E, Cell Biolabs, USA) that were used for retrovirus generation, were cultured in Eagle's Minimum Essential (EME) medium (4.5 g/l glucose, 10 % FBS, 1% penicillin and streptomycin, 1 µg/ml puromycin, 10 µg/ml blasticidin S (all from Sigma-Aldrich, Germany)) in a humidified 5% $CO_2$ atmosphere at 37°C. 16 µg of the retroviral constructs were transfected into Plat-E cells with 48 µg of polyethylenimine MAX (PEI "MAX", Polysciences, USA) according to the manufacturer's protocol. Retrovirus was isolated from cell culture supernatants 48 hours after transfection. Retrovirus was transduced into C2C12 cells using 5 µg/ml polybrene (Santa Cruz, USA) and spinoculation at 800xg for 90 min at 32°C.

**RNA isolation, cDNA synthesis and quantitative real-time PCR**

Total RNA was isolated from skeletal muscle or cultured cells using TRIzol® Reagent

(Invitrogen, USA) according to the manufacturer's protocol. cDNA synthesis of 1 µg of RNA per sample was carried out by using the SuperScript® First-Strand Synthesis System (Invitrogen, USA). Quantitative real-time polymerase chain reaction (qRT-PCR) was performed using Power SYBR® Green PCR Master Mix (Applied Biosystems, USA) and self-designed primers (for primer sequences see Table S6), in a Step-One Plus or a QuantStudio 3 thermocycler (both Applied Biosystems, USA) as described recently using a cDNA standard curve [1, 2]. Gene expression was normalized to the stably expressed glyceraldehyde-3-phosphate dehydrogenase (*Gapdh*).

**Immunostaining of myoblasts and myotubes in vitro**

For immunofluorescence microscopy cells were cultured in IBIDI slides (Ibidi GmbH, Germany), fixed with 4% paraformaldehyde (pH 7.0; 15 min, room temperature), permeabilized with 0.2% Triton X-100 in PBS for 30 min at room temperature, blocked with 5% goat serum (Dako, Germany) for 1 hour at room temperature corresponding to the primary antibodies host and incubated with specific primary antibody overnight at 4°C. After washing with PBS containing 0.2% Tween20 (Carl Roth, Germany), cells were incubated with fluorescent secondary antibody for 1 hour at room temperature in a dark environment. Stained cells were embedded in ProLong Gold® Antifade Reagent that contained DAPI for nuclei staining (Invitrogen, USA). Pictures were taken with a Keyence microscope (BZ-X810, Keyence, Japan) and the Zeiss confocal laser scanning microscope (LSM 980 with Airyscan 2, Carl Zeiss Inc., Germany), and analyzed with BZ-X800 Analyzer (Keyence, Japan) and analysis software (Zen v. 3.3.89, Carl Zeiss Inc., Germany), respectively. Myogenic differentiation index was calculated as the percentage of nuclei in fast MyHC positive myotubes related to the total number of nuclei per field of view. The fusion index was calculated as the percentage of nuclei number in fast MyHC positive myotubes.

**Protein extraction and immunoblotting**

Protein analyses were performed as recently published [1]. Shortly, cells were lysed in radioimmunoprecipitation assay (RIPA) buffer (50 mM Tris HCl, pH 7.5, 150 mM NaCl, 0.5% (w/v) sodium-deoxycholate, 1% (v/v) nonident P-40, 1 mM EDTA (ethylenediaminetetraacetic acid), 0.2% (w/v) sodium dodecyl sulfate (SDS)) containing protease (cOmplete, Roche, Germany) and phosphatase (1 mM $Na_3VO_4$, 1 mM phenylmethylsulfonyl fluoride, PhosSTOP (Roche, Germany)) inhibitors at 4°C. Lysates were cleared by centrifugation (4°C, 10 min, 12,000xg). The supernatant was assayed for protein concentration using the Bradford protein assay (Bio-Rad Laboratories, USA), frozen and stored at -80°C until usage. Proteins were separated by 10% sodium dodecyl sulfate–polyacrylamide gel electrophoresis (SDS-PAGE) and blotted onto nitrocellulose membranes (NC; Amersham Pharmacia Biotech, UK). Membranes were blocked with 5% BSA or 5% dry milk in Tris-buffered saline with 0.1% Tween20 (TBST), then incubated with primary and secondary antibodies as indicated and the signal was visualized with the ChemiDoc™ MP Imaging System (Bio-Rad Laboratories, USA). The ImageLab™ 6.0.1 software (Bio-Rad Laboratories, USA) was used for image analysis. *Protein sample preparation for affinity purification followed by MS analysis:* Cells were grown in 6-well plates or T75 cell culture flasks, and harvested using lysis buffer (10 mM TRIS, 150 mM NaCl, 100 ng/ml cOmplete). Following three freeze&thaw cycles cell membranes were destroyed using a syringe (needle size Ø 0.40 x 20 mm). The supernatant was precleared by low speed centrifugation (10 min, 300xg); resulting supernatants were subjected to high speed centrifugation (20 min, 50,000xg). The clear middle phase was collected for Nickel-NTA (Thermo Fisher Scientific, USA) pull-down and subsequent MS analysis. *Protein sample preparation for mass spectrometry analysis of SNX5-enriched endosomes:* Cell membranes were destroyed using a syringe (needle size Ø 0.40 x 20 mm) in homogenization buffer (250 mM sucrose, 3 mM imidazole, 1 mM EDTA, 0.03 mM cycloheximide, cOmplete and phosphatase inhibitor cocktail 1 and 2) to isolate the post-nuclear supernatant (PNS), in which

endosomes are maintained. The SNX5-coated endosomes were purified from PNS using Pierce™ Protein A/G Agarose (Thermo Fisher Scientific, USA) that was pre-coated with anti-SNX5 antibody overnight at 4°C. Subsequently, SNX5-precipitates were subjected to MS analysis or to other indicated assays. *For nucleus and cytoplasm fractionation:* All preparations were performed on ice. Cytoplasm fractions were obtained from the PNS as indicated. Next, nuclear proteins were isolated in NE-PER™ Nuclear Extraction Reagents (Thermo Fisher Scientific, USA). Nuclei pellets separated from the PNS isolation were resuspended in nuclear lysis buffer for 30 min, 4°C and cleared by centrifugation (4°C, 10 min, 12,000xg).

**Affinity purification and coimmunoprecipitation**

Proteins were isolated from transfected cells using lysis buffer (50 mM potassium-phosphate buffer ($KH_2PO_4$ (pH 4.0)/$K_2HPO_4$ (pH 9.3)), 150 mM NaCl, cOmplete, 0.2% TritonX-100, pH7.4). 10% of cell lysates were used for input controls. Nickel-NTA and anti-FLAG M2 Affinity Gel (Sigma-Aldrich, Germany) were used to precipitate His- and FLAG-tagged proteins, respectively. Proteins from input control and precipitates were subjected to Western blot analysis with the indicated antibodies. *Sample preparation for proteinase K and PNGase F digestion:* The SNX5-coated endosomes were purified from PNS using Pierce™ Protein A/G Agarose that was pre-coated with anti-SNX5 antibody overnight at 4°C. SNX5-precipitates were subjected to proteinase K (New England Biolabs, Germany) digestion. Afterwards, proteinase K was inactivated by 1 hour of PMSF (Sigma-Aldrich, Germany) treatment. SNX5-precipitates were subjected to PNGase F (New England Biolabs, Germany) as indicated referring to the manufacturer's protocol.

**Cycloheximide chase and Ubiquitination assays**

Protein stability assays were performed by exposing transfected cells to cycloheximide (CHX, 100 µg/ml) to inhibit protein synthesis. Proteins were isolated at indicated time points and analyzed by Western blot analyses with indicated antibodies. All CHX experiments were

performed independently and at least twice using biological duplicates each. Representative Western blots and their densitometric analyses are shown.

In vitro ubiquitination assays were performed as recently published [1]. Briefly, COS-7 cells were transfected as indicated for 48 hours. Prior to harvesting, cells were treated with either vehicle (0.25% DMSO) or the proteasome inhibitor MG132 (25 μM) for 6 hours. Cells were lysed in lysis buffer (50 mM potassium-phosphate buffer ($KH_2PO_4$ (pH 4.0)/$K_2HPO_4$ (pH 9.3)), 150 mM NaCl, cOmplete, 25mM N-Ethylmaleimide (NEM, Sigma-Aldrich, Germany), 0.2% TritonX-100, pH7.4) and 10% of the lysates were used for input controls. Lysates were immunoprecipitated (IP) with anti-FLAG M2 affinity gel overnight at 4°C. Proteins from input control and precipitates were subjected to Western blot analyses with the indicated antibodies.

**Cell fractionation and PKA assays**

Sucrose gradient (30%, 40%, 50%, 60% sucrose) fractionation was performed from 400 μl PNS by ultracentrifugation at 130,000xg for 3 hours at 4°C. Nine fractions were collected for Western blot analyses with indicated antibodies. Endosome enriched fractions were isolated from PNS by ultracentrifugation at 120,000xg for 1 hour at 4°C. The supernatant was collected as the cytosol fraction. The membrane-containing pellet was washed with ice cold PBS and resuspended in RIPA buffer. Proteins from the isolated fractions were analyzed by Western blot analyses with indicated antibodies.

PKA activity was measured using the PKA Colorimetric Activity Kit (Thermo Fisher Scientific, USA) according to the manufacturer's instruction.

**Cross-linking experiments**

Cross-linking experiments were performed according to a previously published protocol [3]. Briefly, after treatment, cells were harvested in lysis buffer (20mM, pH7.5 HEPES-KOH, 10 mM KCl, 1.5 mM $MgCl_2$, 1 mM EDTA, 1 mM EGTA (ethylene glycol-bis(β-aminoethyl ether)-N,N,N',N'-tetraacetic acid), and 320 mM sucrose). Following centrifugation, the

supernatant and the pellet were diluted in CHAPS ((3-[(3-cholamidopropyl) dimethylammonio]-1-propanesulfonate)) buffer (20mM, pH7.5 HEPES-KOH, 5 mM $MgCl_2$, 0.5 mM EGTA, 0.1 mM PMSF and 0.1% CHAPS) and then incubated with non-cleavable disuccinimidyl suberate (DSS, 4 mM, Thermo Fisher Scientific, USA) for 30 min at 4°C. After resuspension in Laemmli buffer (Bio-Rad Laboratories, USA), proteins were analyzed by immunoblotting.

**ChIP-qRT-PCR**

Chromatin immunoprecipitation (ChIP) assay was performed according to the manufacturer's protocol using the CUT&RUN Assay Kit (Cell Signaling, USA). Briefly, fixed C2C12 cells were incubated with concanavalin A-coated magnetic beads and permeabilization was performed with digitonin (0.05%)-containing buffer. Afterwards, cells were incubated with anti-MEF2D antibody (1 µg) or anti-tri-methyl-histone H3 (Lys4) (clone C42D8) antibody (0.5 µg) and rabbit IgG antibody (negative control for anti-MEF2D, 1 µg) or rabbit isotype specific IgG antibody (negative control for anti-Histone H3, 0.5 µg) overnight at 4°C. The cell-bead-antibody slurry was incubated with protein A/G-MNase (Protein A and Protein G IgG binding domains fused to micrococcal nuclease) for 1 hour at 4°C. CUT&RUN fragments were released by incubation for 10 min at 37°C followed by centrifugation for 5 min at 16,000xg. Reverse crosslinking of released CUT&RUN fragments was performed in 10% SDS and proteinase K (20mg/ml) at 65°C overnight. An input sample was digested with proteinase K (20 mg/ml) and RNase A at 55°C for 1 hour. Afterwards, the input sample was sonicated (Bioruptor Pico, Diagenode, Belgium) for 35 cycles (30sec ON/ 30 seconds OFF) at 4°C. qPCR with self-generated primers for MEF2D and company provided primers for Histone H3 (Table S4) was used to determine changes in DNA amounts.

**Antibodies**

Following antibodies were used: mouse anti-GAPDH (clone 6C5), rabbit anti-Myc

(both from Merck, Germany), rabbit anti-FLAG, mouse anti-HA, rabbit anti-RI-α, rabbit anti-PKA catalytic subunit, rabbit anti-phospho-CREB (Ser133), rabbit anti-CREB (48H2), rabbit anti-HDAC4, anti-mouse IgG HRP linked, anti-rabbit IgG HRP linked (all from Cell Signaling, USA), mouse anti-Myc, mouse anti-myosin (slow, NOQ7), mouse anti-myosin (fast, My32), mouse anti-myogenin (all from Sigma-Aldrich, Germany), rabbit anti-SNX5, rabbit anti-Myostatin (GDF8), rabbit anti-RAB5 (RAB5A) (all from Proteintech, UK), rabbit anti-LaminB1, rabbit anti-Histone H3 (both from Abcam, UK), mouse anti-MEF2D, mouse anti-EEA1, mouse anti-LAMP1 (all from BD Biosciences, USA), rabbit anti-MuRF2, rabbit anti-MuRF3 (own production[2]), anti-mouse Alexa Fluor®488, anti-rabbit Alexa Fluor®488, anti-mouse Alexa Fluor®555, anti-rabbit Alexa Fluor®555, and anti-mouse Alexa Fluor®647 (all from Life Technologies, USA).

**Mass spectrometric analysis**

*Determination of MuRF3 interaction partners:* precipitates containing MuRF3 and protein-interaction partners were resuspended in 100 µl denaturation buffer (10mM HEPES, pH 8.0, 6M urea, 2M thiourea). Disulfide bonds were reduced with 10 mM tris(2-carboxyethyl) phosphine (TCEP) and cysteine groups were alkylated with 55 mM 2-chloroacetamide (CAA). The proteins were digested with Lys-C overnight. Peptides were extracted, desalted and stored on reversed-phase (C18) StageTips [4]. The SILAC labelled IP pairs were mixed prior to the MS analysis. *High throughput LC-MS/MS analysis:* After Stage-Tip extraction, the eluted peptides were lyophilized and resuspended in 3% trifluoroacetic acid/5% acetonitrile. Peptides were separated on a Proxeon nLC-II system (Thermo Fisher Scientific, USA), resolved with a reversed-phase column (Dr. Maisch GmbH C18) by a gradient from 4 to 42% acetonitrile in 240 min. MS and MS/MS spectra were recorded on a QExactive mass spectrometer (Thermo Fisher Scientific, USA). The mass spectrometer was operated in a data-dependent acquisition mode with dynamic exclusion enabled (30s). Survey scans (mass range 300-1500 Th) were

acquired at a resolution of 70,000, with the twenty most abundant multiply charged ($z \geqslant 2$) ions selected with a 3-Th isolation window for HCD fragmentation. MS/MS scans were acquired at a resolution of 35,000 and injection time of 120ms, ACG 10e5. Processing of mass spectrometry data: protein and peptide quantitation information were extracted from MaxQuant 1.2.2.5 [5]. Results were filtered to 1% false discovery rate (FDR) at peptide and protein level by MaxQuant. Variable modifications were set to oxidation of methionines and fixed modifications were set to carbamidomethylation of cysteines. The SILAC parameters were set to light and heavy labelling on lysine (+8Da). Additionally, the match between runs and the requantify option were activated. Further analysis was performed using the R-statistical language (www.R-project.org). *Determination of proteins contained in SNX5 precipitates:* Sepharose with precipitated SNX5 and interacting proteins were reconstituted in 30 µl Tris-HCl buffer (pH 8.0, 50 mM) containing 10 mM dithiotreitol (DTT) and 2% SDS. Samples were heated at 95°C for 5 min and the protein containing supernatant was collected after centrifugation (5 min, 13,800xg). Ten µl sample was subjected to a bead based SP3 protocol applied for protein digestion and peptide purification [6]. The resulting peptides were separated by Liquid chromatography (LC; Ultimate 3000, Thermo Electron, Germany) before data-dependent acquisition of MS data on a Q Exactive Plus mass spectrometer (Thermo Electron, Germany). MS data were analyzed in Proteome discoverer 2.3 (Thermo Electron, Germany). Cysteine carbamidomethylation was set as static modification, oxidation at methionine and acetylation at protein N-terminus were defined as variable modifications, and up to two missed cleavages were allowed. Proteins were only considered for further analyses, when identified by at least one unique peptide (FDR<0.05). Further details are provided in Table S7. The mass spectrometry proteomics data have been deposited to the ProteomeXchange Consortium via the PRIDE [7] partner repository with the dataset identifiers PXD058900 (MuRF3 interaction partners) and PXD057619 (proteins contained in SNX5 precipitates).

**References for Supplementary Methods section**

1. Li Y, Dormann N, Brinschwitz B, Kny M, Martin E, Bartels K, et al. SPSB1-mediated inhibition of TGF-beta receptor-II impairs myogenesis in inflammation. J Cachexia Sarcopenia Muscle. 2023;14:1721-36.

2. Lodka D, Pahuja A, Geers-Knorr C, Scheibe RJ, Nowak M, Hamati J, et al. Muscle RING-finger 2 and 3 maintain striated-muscle structure and function. J Cachexia Sarcopenia Muscle. 2016;7:165-80.

3. Fernandes-Alnemri T, Wu J, Yu JW, Datta P, Miller B, Jankowski W, et al. The pyroptosome: a supramolecular assembly of ASC dimers mediating inflammatory cell death via caspase-1 activation. Cell Death Differ. 2007;14:1590-604.

4. Rappsilber J, Mann M, Ishihama Y. Protocol for micro-purification, enrichment, pre-fractionation and storage of peptides for proteomics using StageTips. Nat Protoc. 2007;2:1896-906.

5. Cox J, Mann M. MaxQuant enables high peptide identification rates, individualized p.p.b.-range mass accuracies and proteome-wide protein quantification. Nat Biotechnol. 2008;26:1367-72.

6. Sielaff M, Kuharev J, Bohn T, Hahlbrock J, Bopp T, Tenzer S, et al. Evaluation of FASP, SP3, and iST Protocols for Proteomic Sample Preparation in the Low Microgram Range. J Proteome Res. 2017;16:4060-72.

7. Perez-Riverol Y, Bai J, Bandla C, Garcia-Seisdedos D, Hewapathirana S, Kamatchinathan S, et al. The PRIDE database resources in 2022: a hub for mass spectrometry-based proteomics evidences. Nucleic Acids Res. 2022;50:D543-D52.

**Supplementary References**

S1. Lange S, Xiang F, Yakovenko A, Vihola A, Hackman P, Rostkova E, et al. The kinase domain of titin controls muscle gene expression and protein turnover. Science. 2005;308:1599-

603.

S2. Witt CC, Witt SH, Lerche S, Labeit D, Back W, Labeit S. Cooperative control of striated muscle mass and metabolism by MuRF1 and MuRF2. EMBO J. 2008;27:350-60.

S3. Willis MS, Wadosky KM, Rodriguez JE, Schisler JC, Lockyer P, Hilliard EG, et al. Muscle ring finger 1 and muscle ring finger 2 are necessary but functionally redundant during developmental cardiac growth and regulate E2F1-mediated gene expression in vivo. Cell Biochem Funct. 2014;32:39-50.

S4. Bodine SC, Latres E, Baumhueter S, Lai VK, Nunez L, Clarke BA, et al. Identification of ubiquitin ligases required for skeletal muscle atrophy. Science. 2001;294:1704-8.

S5. Ong SE, Blagoev B, Kratchmarova I, Kristensen DB, Steen H, Pandey A, et al. Stable isotope labeling by amino acids in cell culture, SILAC, as a simple and accurate approach to expression proteomics. Mol Cell Proteomics. 2002;1:376-86.

S6. Mann M. Functional and quantitative proteomics using SILAC. Nat Rev Mol Cell Biol. 2006;7:952-8.

S7. Kvainickas A, Jimenez-Orgaz A, Nagele H, Hu Z, Dengjel J, Steinberg F. Cargo-selective SNX-BAR proteins mediate retromer trimer independent retrograde transport. J Cell Biol. 2017;216:3677-93.

S8. Pan T, Gao S, Cui X, Wang L, Yan S. APC/CCDC20 targets SCFFBL17 to activate replication stress responses in Arabidopsis. Plant Cell. 2023;35:910-23.

S9. Da Graca J, Morel E. Canonical and Non-Canonical Roles of SNX1 and SNX2 in Endosomal Membrane Dynamics. Contact (Thousand Oaks). 2023;6:25152564231217867.

S10. Kwon SH, Oh S, Nacke M, Mostov KE, Lipschutz JH. Adaptor Protein CD2AP and L-type Lectin LMAN2 Regulate Exosome Cargo Protein Trafficking through the Golgi Complex. J Biol Chem. 2016;291:25462-75.

S11. Grade CVC, Mantovani CS, Alvares LE. Myostatin gene promoter: structure, conservation and importance as a target for muscle modulation. J Anim Sci Biotechnol. 2019;10:32.

S12. Moriscot AS, Baptista IL, Bogomolovas J, Witt C, Hirner S, Granzier H, et al. MuRF1 is a muscle fiber-type II associated factor and together with MuRF2 regulates type-II fiber trophicity and maintenance. J Struct Biol. 2010;170:344-53.

S13. Otsuki T, Kajigaya S, Ozawa K, Liu JM. SNX5, a new member of the sorting nexin family, binds to the Fanconi anemia complementation group A protein. Biochem Biophys Res Commun. 1999;265:630-5.

S14. Greig J, Bates GT, Yin DI, Briant K, Simonetti B, Cullen PJ, et al. CHC22 clathrin recruitment to the early secretory pathway requires two-site interaction with SNX5 and p115. EMBO J. 2024 Oct;43(19):4298-4323.

S15. Hara S, Kiyokawa E, Iemura S, Natsume T, Wassmer T, Cullen PJ, et al. The DHR1 domain of DOCK180 binds to SNX5 and regulates cation-independent mannose 6-phosphate receptor transport. Mol Biol Cell. 2008;19:3823-35.

S16. Ghasemizadeh A, Christin E, Guiraud A, Couturier N, Abitbol M, Risson V, et al. MACF1 controls skeletal muscle function through the microtubule-dependent localization of extra-synaptic myonuclei and mitochondria biogenesis. Elife. 2021;10:e70490.

S17. Im SK, Jeong H, Jeong HW, Kim KT, Hwang D, Ikegami M, et al. Disruption of sorting nexin 5 causes respiratory failure associated with undifferentiated alveolar epithelial type I cells in mice. PLoS One. 2013;8:e58511.

S18. Hierro A, Gershlick DC, Rojas AL, Bonifacino JS. Formation of Tubulovesicular Carriers from Endosomes and Their Fusion to the trans-Golgi Network. Int Rev Cell Mol Biol. 2015;318:159-202.

S19. Pizon V, Rybina S, Gerbal F, Delort F, Vicart P, Baldacci G, et al. MURF2B, a novel LC3-binding protein, participates with MURF2A in the switch between autophagy and ubiquitin proteasome system during differentiation of C2C12 muscle cells. PLoS One. 2013;8:e76140.

S20. Gupte RS, Weng Y, Liu L, Lee MY. The second subunit of the replication factor C

311 complex (RFC40) and the regulatory subunit (RIalpha) of protein kinase A form a protein
312 complex promoting cell survival. Cell Cycle. 2005;4:323-9.
313 S21. Backs J, Worst BC, Lehmann LH, Patrick DM, Jebessa Z, Kreusser MM, et al. Selective
314 repression of MEF2 activity by PKA-dependent proteolysis of HDAC4. J Cell Biol.
315 2011;195:403-15.
316 S22. Lu J, McKinsey TA, Zhang CL, Olson EN. Regulation of skeletal myogenesis by
317 association of the MEF2 transcription factor with class II histone deacetylases. Mol Cell.
318 2000;6:233-44.
319 S23. He T, Huang J, Chen L, Han G, Stanmore D, Krebs-Haupenthal J, et al. Cyclic AMP
320 represses pathological MEF2 activation by myocyte-specific hypo-phosphorylation of HDAC5.
321 J Mol Cell Cardiol. 2020;145:88-98.
322
323 **Supplementary Tables**
324 **Table S1. Primers crRNA targeting SNX5 and for generation of cDNA expression**
325 **plasmids.**

| **Primer Name (restriction site)** | **Oligonucleotide sequence (5'-3')** |
|---|---|
| SNX5-targeted crRNA | ACUGAAACAACGGAU |
| MuRF1 Flag for (EcoRI) | GCGAATTCGATTATAAATCTAGCCTGA |
| MuRF1 Flag rev (ApaI) | GCGGGCCCTCATTGGTGTTCTTCTTT |
| MuRF2 Flag for (ClaI) | GCATCGATAGCACTTCTCTGAATTACAAGTCTT |
| MuRF2 Flag rev (ApaI) | GCGGGCCCTTATTCATTTAGGGAATT |
| MuRF3 Flag for (EcoRI) | GCGAATTCAACTTCACGGTGGGTTTCAA |
| MuRF3 Flag rev (ApaI) | GCGGGCCCTCAGTGCAGGCCTGAGCCTTC |
| SNX5 His/Myc for (BamHI) | CGGGATCCATGGCCGCGGTTCCCGAGTT |
| SNX5 His/Myc rev (KpnI) | GGGGTACCGTTGTTCTTGAATAAGTCGATGCAGCTC |

| | |
|---|---|
| SNX5 Flag for (ClaI) | CCATCGATGCCGCGGTTCCCGA |
| SNX5 Flag rev (XbaI) | GCTCTAGATCAGTTGTTCTTGAATAAGTCGATGC |
| MuRF1 His/Myc for (EcoRI) | CAGAATTCATGGATTATAAATCTAGCCTG |
| MuRF1 His/Myc rev (KpnI) | CTTGGTACCTTGGTGTTCTTCTTTACCCTC |
| MuRF2 His/Myc for (XhoI) | GACTCGAGATGAGCACTTCTCTGAATTAC |
| MuRF2 His/Myc rev (KpnI) | CTTGGTACCTTCATTTAGGGAATTCAACCAG |
| MuRF3 His/Myc for (XbaI) | TCTAGACTATGAACTTCACGGTGGGTTTCAA |
| MuRF3 His/Myc rev (KpnI) | GGTACCGTGCAGGCCTGAGCCTTCTGGCAC |

326

| Protein IDs | Protein Names | Gene Names | Uniprot | Ratio M/L Normalized MSC04526 | Ratio M/L Normalized MSC04526 Significance B |
|---|---|---|---|---|---|
| IPI00457401;I | Transmembrane BAX inhibitor motif-containing | Tmbim6 | Q9D2C7;E0CX98;E0CXR0; | 7,330 | 1,646E-16 |
| IPI00652882;I | Protein fat-free homolog | Ffr | Q3UVL4-1;Q3UVL4;Q3UVL | 4,572 | 4,139E-07 |
| IPI00830533;I | Tropomyosin-1 | Tpm1 | E9Q454;P58771-1;P58771 | 4,541 | 3,006E-09 |
| IPI00331708;I | Myocardin-related transcription factor A | Mkl1 | Q8K4J6-1;Q8K4J6;Q3U1I6 | 4,108 | 5,991E-06 |
| IPI00406306;I | Tumor suppressor p53 | P53 | P02340;O70366;Q549C9;( | 3,586 | 8,696E-05 |
| IPI00120617;I | AN1-type zinc finger protein 2A | Airap | Q9JII7;D3YUL0 | 3,425 | 5,317E-08 |
| IPI00125454;I | DnaJ homolog subfamily A member 4 | Dnaja4 | Q9JMC3;Q8R1X2 | 3,402 | 6,639E-08 |
| IPI00125140 | Activity-regulated cytoskeleton-associated prote | Arc | Q9WV31 | 3,053 | 9,348E-04 |
| IPI00308785;I | Cyclooxygenase-2 | Cox2 | Q05769;Q3UMR6;Q543K3; | 2,978 | 1,268E-03 |
| IPI00346073;I | Heat shock 70 kDa protein 1 | Hsp70a1 | P17879;A1E2B8;Q61698 | 2,978 | 3,668E-05 |
| IPI00989436;I | HCV NS5A-transactivated protein 9 homolog | Ns5atp9 | Q9CQX4 | 2,873 | 1,925E-03 |
| IPI00138274;I | Alpha(B)-crystallin | Crya2 | P23927;Q52L78;E9QMA0 | 2,867 | 6,884E-06 |
| IPI00128522;I | Heat shock 25 kDa protein | Hsp25 | P14602-1;P14602;Q545F4 | 2,866 | 6,960E-06 |
| IPI00113117 | CCN family member 1 | Ccn1 | P18406;Q3TX21 | 2,848 | 8,171E-05 |
| IPI00322594 | CCN family member 2 | Ccn2 | P29268;Q91V29 | 2,825 | 9,599E-06 |
| IPI00626662;I | Aldehyde dehydrogenase family 1 member A1 | Ahd2 | P24549 | 2,738 | 1,878E-05 |
| IPI00331564;I | Dihydrolipoyl dehydrogenase | Dld | Q3TIE8;O08749 | 2,730 | 3,319E-03 |
| IPI00108058 | CDK-interacting protein 1 | Cdkn1a | P39689;Q4FK34;Q564P6 | 2,701 | 1,947E-04 |
| IPI00132942 | Nuclear distribution protein C homolog | Nudc | O35685;A2A9F5 | 2,615 | 8,901E-04 |
| IPI00987945;I | SRY-box containing gene 9 | Sox9 | Q571J2;Q04887;B1AVH1;( | 2,592 | 5,525E-05 |
| IPI00136253;I | DnaJ (Hsp40) homolog, subfamily B, member 1 | Dnajb1 | Q9QYJ3;Q3TIT6;Q3TU79;( | 2,591 | 3,624E-04 |
| IPI00515257;I | RNA polymerase B transcription factor 3 | Btf3 | Q64152-1;Q64152;Q6415 | 2,574 | 3,965E-04 |
| IPI00124640 | Acrogranin | Grn | P28798;Q3TVQ3;Q3TW77; | 2,572 | 5,884E-03 |
| IPI00117689;I | Cavin-1 | Ptrf | O54724 | 2,547 | 4,601E-04 |
| IPI00120984 | NADH dehydrogenase [ubiquinone] 1 alpha sub | Ndufa8 | Q9DCJ5 | 2,537 | 6,646E-03 |
| IPI00132958 | Acyl-coenzyme A thioesterase 13 | Acot13 | Q9CQR4;Q4VA32 | 2,530 | 1,331E-03 |
| IPI00131577;I | Heme oxygenase 1 | Hmox1 | P14901;Q3U5H8;Q3U5U6; | 2,517 | 5,421E-04 |
| IPI00132539 | Basic transcription factor 3-like 4 | Btf3l4 | Q9CQH7;A2A7Z4;Q78IG7 | 2,492 | 1,595E-03 |
| IPI00110370;I | Tissue inhibitor of metalloproteinases 3 | Timp3 | P39876;Q54AE5;Q6GXA7 | 2,487 | 1,161E-04 |
| IPI00131620;I | DNA polymerase kappa | Dinb1 | Q9QUG2-1;Q9QUG2;Q5Q9 | 2,433 | 9,485E-03 |
| IPI00110760 | DnaJ homolog subfamily B member 4 | Dnajb4 | Q9D832 | 2,403 | 2,393E-03 |
| IPI00453954 | Transcription elongation factor A protein-like 8 | Tceal8 | Q9CZY2 | 2,366 | 2,815E-03 |
| IPI00421223 | Tropomyosin-4 | Tpm4 | Q6IRU2 | 2,363 | 2,855E-03 |
| IPI00752148;I | C9orf119 homolog | 2900010J23Rik | Q8K3D3-2;Q8K3D3;Q8K3I | 2,351 | 2,899E-04 |
| IPI00111793;I | Entactin | Ent | P10493;Q3TKX9 | 2,326 | 1,350E-02 |
| IPI00119202;I | Calgizzarin | S100a11 | P50543 | 2,193 | 2,802E-03 |
| IPI00399972;I | Transforming acidic coiled-coil-containing prote | Tacc1 | Q6Y685-1;Q6Y685;Q6Y68 | 2,172 | 2,183E-02 |
| IPI00112347 | Inhibin beta A chain | Inhba | Q04998;Q3UXL8;Q3UY39; | 2,156 | 6,891E-03 |
| IPI00320462 | Biphenyl hydrolase-like protein | Bphl | Q8R164;Q3TDN8 | 2,153 | 2,317E-02 |
| IPI00263863;I | Heat shock protein 1 (Chaperonin 10) | Hspe1 | Q64433;Q4KL76;Q9JI95 | 2,086 | 9,122E-03 |
| IPI00678003;I | Inosine triphosphate pyrophosphatase | Itpa | Q9D892;Q60I30;Q3U589 | 2,051 | 3,134E-02 |
| IPI00130225 | Sorting nexin-4 | Snx4 | Q91YJ2;Q80X54 | 2,035 | 1,112E-02 |
| IPI00173343 | Oligoribonuclease, mitochondrial | Rexo2 | Q9D8S4;Q3T9B4;Q3TAV0; | 2,035 | 1,113E-02 |
| IPI00403336;I | Optic atrophy protein 1 | Opa1 | P58281-2;P58281;Q8BK9 | 2,029 | 2,075E-03 |
| IPI00125899;I | Beta-catenin | Ctnnb1 | Q02248;Q3UZT7;Q80VE7; | 2,021 | 1,172E-02 |
| IPI00170101 | Optineurin | Optn | Q8K3K8 | 2,018 | 3,444E-02 |
| IPI00228343 | Ferrochelatase, mitochondrial | Fech | P22315;Q3UC49;Q544X6;( | 1,982 | 2,703E-03 |
| IPI00132903 | Ubiquitin-fold modifier-conjugating enzyme 1 | Ufc1 | Q9CR09 | 1,947 | 1,556E-02 |
| IPI00625105;I | U1 small nuclear ribonucleoprotein 70 kDa | Snrnp70 | Q62376-1;Q62376;A2RS6 | 1,928 | 4,433E-02 |
| IPI00132208;I | DnaJ homolog subfamily A member 1 | Dnaja1 | P63037;Q3TK61;Q5NTY0;I | 1,907 | 1,005E-02 |
| IPI00316740;I | Damage-specific DNA-binding protein 1 | Ddb1 | Q3U1J4;Q91YC8;Q3ULS8 | 1,897 | 4,828E-02 |
| IPI00112053 | Sorting nexin-5 | Snx5 | Q9D8U8;A2ANA4;Q3TJN6; | 1,870 | 2,062E-02 |
| IPI00830178;I | Angiomotin | Amot | Q8VHG2-1;Q8VHG2;Q8VH | 1,846 | 2,247E-02 |
| IPI00121427 | S100 calcium-binding protein A6 | S100a6 | P14069;Q545I9 | 1,845 | 1,300E-02 |
| IPI00606184;I | Zinc finger protein 703 | Znf703 | P0CL69 | 1,838 | 2,305E-02 |
| IPI00331318;I | Palmitoyl-protein hydrolase 1 | Ppt1 | O88531;Q3TAR8;Q3U6J9;( | 1,835 | 5,928E-03 |
| IPI00322530;I | Acyl-CoA desaturase 1 | Scd1 | P13516;Q3UXG5;Q547C4; | 1,823 | 2,433E-02 |
| IPI00469329;I | 3-hydroxy-3-methylglutaryl-coenzyme A reduct | Hmgcr | Q01237;Q6PB59;Q8BV96; | 1,806 | 2,586E-02 |
| IPI00675897 | Muscle-specific RING finger protein 2 | Trim55 | Q8C6Y1 | 1,804 | 2,602E-02 |
| IPI00381563;I | Cytospin-B | Cytsb | Q5SXY1-3;Q5SXY1;Q5SXY | 1,799 | 2,647E-02 |
| IPI00850843;I | AHNAK Nucleoprotein 2 | Ahnak2 | E9PYB0;Q3UUE0 | 1,754 | 3,096E-02 |
| IPI00114209;I | Glutamate dehydrogenase 1, mitochondrial | Glud1 | P26443;Q3TSQ7 | 1,732 | 2,034E-02 |
| IPI00124751;I | Transient receptor potential cation channel subf | Trpc4ap | Q9JLV2-1;Q9JLV2;Q3TB80 | 1,692 | 3,805E-02 |
| IPI00310323;I | Retinoid-inducible serine carboxypeptidase | Scpep1 | Q920A5;Q9D625;Q99J29 | 1,686 | 3,882E-02 |
| IPI00111218;I | Aldehyde dehydrogenase 2, mitochondrial, isofo | Aldh2 | P47738;Q3TVM2;Q3U6I3;( | 1,658 | 2,685E-02 |
| IPI00338785;I | Laminin B1 | Lamb-1 | P02469;B9EKB0;E9QN70;( | 1,645 | 4,438E-02 |
| IPI00830443;I | Caseinolytic peptidase B protein homolog | Clpb | E9PY58;Q3TXD4;Q3U3U6; | 1,636 | 1,571E-02 |
| IPI00230476;I | Diaphanous-related formin-3 | Diap3 | Q9Z207;Q3TSX1;Q3UU77; | 1,631 | 1,609E-02 |
| IPI00776049;I | Translation initiation factor IF-2 | Mtif2 | Q5M6W6;Q91YJ5;Q5M6W7 | 1,609 | 4,977E-02 |
| IPI00453812 | CTTNBP2 N-terminal-like protein | Cttnbp2nl | Q99LJ0;Q922L8 | 1,588 | 1,961E-02 |
| IPI00122362 | Protein disulfide isomerase-related protein | Pdia5 | Q921X9;Q9CSM8 | 1,574 | 2,084E-02 |
| IPI00135660 | Cavin-2 | Sdpr | Q63918 | 1,555 | 2,273E-02 |
| IPI00226430;I | Acetyl-CoA acyltransferase | Acaa2 | Q8BWT1;Q3TIT9;Q3UKH3 | 1,548 | 4,000E-02 |
| IPI00928513;I | Interferon-related developmental regulator 1 | Ifrd1 | Q80XM4;P19182;E9Q949; | 1,538 | 2,449E-02 |
| IPI00126072 | Vesicle amine transport protein 1 homolog (T ca | Vat1 | Q62465;Q3TXD3;Q3U331; | 1,527 | 2,567E-02 |
| IPI00116753 | Electron transfer flavoprotein subunit alpha, mit | Etfa | Q99LC5;B1B1B4 | 1,517 | 2,687E-02 |
| IPI00128671;I | Cyclin-A2 | Ccna2 | P51943;Q8BRG1;D6RIK7 | 1,516 | 2,694E-02 |
| IPI00129517;I | Peroxiredoxin-5, mitochondrial | Prdx5 | P99029-1;P99029;Q3U7H9 | 1,498 | 2,906E-02 |
| IPI00985904;I | Mediator complex subunit 15 | Med15 | Q3TE00;E9Q7C1;Q6KAM1; | 1,464 | 3,358E-02 |
| IPI00396833;I | Tyrosine--tRNA ligase | Yars2 | Q8BYL4 | 1,432 | 3,847E-02 |
| IPI00319830;I | Beta-II spectrin | Spnb2 | Q62261-1;Q62261;Q8BQ3 | 1,431 | 3,858E-02 |
| IPI00170126;I | Pitrilysin metalloproteinase 1 | Pitrm1 | Q8K411-1;Q8K411;Q8K41 | 1,407 | 4,248E-02 |
| IPI00410836;I | Flap endonuclease 1 | Fen1 | E9PYV9;Q3TGH6;Q8C5X6; | 1,397 | 4,427E-02 |
| IPI00310862;I | Discs large homolog 7 | Dlg7 | Q8K4R9-1;Q8K4R9;Q8K4R | 1,378 | 4,775E-02 |
| IPI00230395;I | Annexin A1 | Anxa1 | P10107;B7STB7;Q3U5N9;( | 1,373 | 4,877E-02 |

Supplementary Table 2

| Accession | Protein name | MB1 SNX vs Gapdh10 | MB2 SNX vs Gapdh11 |
|---|---|---|---|
| Q9JLQ0 | CD2-associated protein OS=Mus musculus OX=10090 GN=Cd2ap PE=1 SV=3 | 3024,58 | 2120,95 |
| Q9DBC7 | cAMP-dependent protein kinase type I-alpha regulatory subunit OS=Mus musculus OX=10090 GN= | 1906,24 | 157,08 |
| Q9CWK8 | Sorting nexin-2 OS=Mus musculus OX=10090 GN=Snx2 PE=1 SV=2 | 1496,56 | 530,67 |
| P97793 | ALK tyrosine kinase receptor OS=Mus musculus OX=10090 GN=Alk PE=1 SV=2 | 1493,39 | 1012,87 |
| Q91YL3 | Uridine-cytidine kinase-like 1 OS=Mus musculus OX=10090 GN=Uckl1 PE=1 SV=1 | 1350,58 | 79,52 |
| B1AVZ0 | Uracil phosphoribosyltransferase homolog OS=Mus musculus OX=10090 GN=Uprt PE=1 SV=1 | 1097,46 | 225,43 |
| Q9QZQ1 | Afadin OS=Mus musculus OX=10090 GN=Afdn PE=1 SV=3 | 1097,05 | 1936,26 |
| Q9DBJ8 | Sorting nexin-5 OS=Mus musculus OX=10090 GN=Snx5 PE=1 SV=1 | 830,50 | 263,74 |
| Q8R050 | Eukaryotic peptide chain release factor GTP-binding subunit ERF3A OS=Mus musculus OX=10090 G | 790,76 | 121,09 |
| Q99MR6 | Serrate RNA effector molecule homolog OS=Mus musculus OX=10090 GN=Srt PE=1 SV=1 | 763,35 | 33,23 |
| P97496 | SWI/SNF complex subunit SMARCC1 OS=Mus musculus OX=10090 GN=Smarcc1 PE=1 SV=2 | 751,59 | 31,82 |
| Q621B8 | Dihydropyrimidinase-related protein 3 OS=Mus musculus OX=10090 GN=Dpysl3 PE=1 SV=1 | 696,63 | 631,25 |
| Q9JJG0 | Transforming acidic coiled-coil-containing protein 2 OS=Mus musculus OX=10090 GN=Tacc2 PE=1 S | 674,03 | 448,98 |
| P55194 | SH3 domain-binding protein 1 OS=Mus musculus OX=10090 GN=Sh3bp1 PE=1 SV=3 | 570,38 | 813,22 |
| Q5F226 | Protocadherin Fat 2 OS=Mus musculus OX=10090 GN=Fat2 PE=1 SV=1 | 535,57 | 1801,48 |
| Q02105 | Complement C1q subcomponent subunit C OS=Mus musculus OX=10090 GN=C1qc PE=1 SV=2 | 484,07 | 683,38 |
| P32261 | Antithrombin-III OS=Mus musculus OX=10090 GN=Serpinc1 PE=1 SV=1 | 452,50 | 512,72 |
| P52430 | Serum paraoxonase/arylesterase 1 OS=Mus musculus OX=10090 GN=Pon1 PE=1 SV=2 | 396,00 | 726,65 |
| Q6PAR5 | GTPase-activating protein and VPS9 domain-containing protein 1 OS=Mus musculus OX=10090 GN= | 320,22 | 93,65 |
| Q62086 | Serum paraoxonase/arylesterase 2 OS=Mus musculus OX=10090 GN=Pon2 PE=1 SV=2 | 316,25 | 442,78 |
| Q9WV80 | Sorting nexin-1 OS=Mus musculus OX=10090 GN=Snx1 PE=1 SV=1 | 289,30 | 653,97 |
| O08638 | Myosin-11 OS=Mus musculus OX=10090 GN=Myh11 PE=1 SV=1 | 282,33 | 411,55 |
| Q6ZQ03 | Formin-binding protein 4 OS=Mus musculus OX=10090 GN=Fnbp4 PE=1 SV=2 | 268,95 | 164,27 |
| P19221 | Prothrombin OS=Mus musculus OX=10090 GN=F2 PE=1 SV=1 | 225,38 | 389,62 |
| Q7TME2 | Sperm-associated antigen 5 OS=Mus musculus OX=10090 GN=Spag5 PE=1 SV=1 | 210,76 | 241,07 |
| O88783 | Coagulation factor V OS=Mus musculus OX=10090 GN=F5 PE=1 SV=1 | 196,96 | 158,54 |
| Q80WV3 | Carbohydrate sulfotransferase 2 OS=Mus musculus OX=10090 GN=Chst2 PE=2 SV=3 | 190,42 | 265,90 |
| Q99PM9 | Uridine-cytidine kinase 2 OS=Mus musculus OX=10090 GN=Uck2 PE=1 SV=1 | 186,24 | 5,82 |
| Q8C804 | Spindle and centriole-associated protein 1 OS=Mus musculus OX=10090 GN=Spice1 PE=1 SV=2 | 172,34 | 171,96 |
| Q9DCZ4 | MICOS complex subunit Mic26 OS=Mus musculus OX=10090 GN=Apoo PE=1 SV=2 | 170,49 | 227,05 |
| Q9QWY8 | Arf-GAP with SH3 domain, ANK repeat and PH domain-containing protein 1 OS=Mus musculus OX= | 150,84 | 166,52 |
| A2RSJ4 | UHRF1-binding protein 1-like OS=Mus musculus OX=10090 GN=Uhrf1bp1l PE=1 SV=2 | 145,76 | 333,03 |
| P52623 | Uridine-cytidine kinase 1 OS=Mus musculus OX=10090 GN=Uck1 PE=1 SV=2 | 128,67 | 20,68 |
| Q3UYV9 | Nuclear cap-binding protein subunit 1 OS=Mus musculus OX=10090 GN=Ncbp1 PE=1 SV=2 | 125,81 | 21,82 |
| P25976 | Nucleolar transcription factor 1 OS=Mus musculus OX=10090 GN=Ubtf PE=1 SV=1 | 115,65 | 13,47 |
| P27641 | X-ray repair cross-complementing protein 5 OS=Mus musculus OX=10090 GN=Xrcc5 PE=1 SV=4 | 103,47 | 7,31 |
| Q4VBE8 | WD repeat-containing protein 18 OS=Mus musculus OX=10090 GN=Wdr18 PE=1 SV=1 | 102,56 | 22,39 |
| P67778 | Prohibitin OS=Mus musculus OX=10090 GN=Phb PE=1 SV=1 | 100,86 | 47,88 |
| Q8R550 | SH3 domain-containing kinase-binding protein 1 OS=Mus musculus OX=10090 GN=Sh3kbp1 PE=1 S | 97,79 | 660,85 |
| Q9DAW6 | U4/U6 small nuclear ribonucleoprotein Prp4 OS=Mus musculus OX=10090 GN=Prpf4 PE=1 SV=1 | 93,53 | 10,02 |
| Q3UQJ9 | Probable ubiquitin carboxyl-terminal hydrolase MINDY-4 OS=Mus musculus OX=10090 GN=Mindy4 | 92,18 | 276,32 |
| Q9R0I7 | YLP motif-containing protein 1 OS=Mus musculus OX=10090 GN=Ylpm1 PE=2 SV=2 | 89,57 | 653,10 |
| P06684 | Complement C5 OS=Mus musculus OX=10090 GN=C5 PE=1 SV=2 | 78,73 | 14,71 |
| P54276 | DNA mismatch repair protein Msh6 OS=Mus musculus OX=10090 GN=Msh6 PE=1 SV=3 | 76,30 | 10,80 |
| E9Q557 | Desmoplakin OS=Mus musculus OX=10090 GN=Dsp PE=1 SV=1 | 73,25 | 231,32 |
| Q8K0V4 | CCR4-NOT transcription complex subunit 3 OS=Mus musculus OX=10090 GN=Cnot3 PE=1 SV=1 | 65,70 | 39,79 |
| Q62191 | E3 ubiquitin-protein ligase TRIM21 OS=Mus musculus OX=10090 GN=Trim21 PE=1 SV=1 | 57,80 | 19,48 |
| Q99KW3 | TRIO and F-actin-binding protein OS=Mus musculus OX=10090 GN=Triobp PE=1 SV=3 | 56,28 | 334,02 |
| Q4KWH5 | 1-phosphatidylinositol 4,5-bisphosphate phosphodiesterase eta-1 OS=Mus musculus OX=10090 GN | 54,75 | 10,68 |
| O08553 | Dihydropyrimidinase-related protein 2 OS=Mus musculus OX=10090 GN=Dpysl2 PE=1 SV=2 | 54,12 | 59,53 |
| Q811S7 | Upstream-binding protein 1 OS=Mus musculus OX=10090 GN=Ubp1 PE=1 SV=1 | 53,53 | 7,14 |
| Q91X43 | SH3 domain-containing protein 19 OS=Mus musculus OX=10090 GN=Sh3d19 PE=1 SV=2 | 52,12 | 63,87 |
| Q4U2R1 | E3 ubiquitin-protein ligase HERC2 OS=Mus musculus OX=10090 GN=Herc2 PE=1 SV=3 | 49,53 | 280,17 |
| Q3TMW1 | Coiled-coil domain-containing protein 102A OS=Mus musculus OX=10090 GN=Ccdc102a PE=1 SV=2 | 48,72 | 629,41 |
| P70255 | Nuclear factor 1 C-type OS=Mus musculus OX=10090 GN=Nfic PE=1 SV=1 | 48,06 | 7,79 |
| P43275 | Histone H1.1 OS=Mus musculus OX=10090 GN=Hist1h1a PE=1 SV=2 | 47,88 | 66,09 |
| P11103 | Poly [ADP-ribose] polymerase 1 OS=Mus musculus OX=10090 GN=Parp1 PE=1 SV=3 | 45,98 | 275,15 |
| Q9CQ49 | Nuclear cap-binding protein subunit 2 OS=Mus musculus OX=10090 GN=Ncbp2 PE=1 SV=1 | 45,11 | 9,92 |
| P97386 | DNA ligase 3 OS=Mus musculus OX=10090 GN=Lig3 PE=1 SV=2 | 43,27 | 12,20 |
| Q9Z1N5 | Spliceosome RNA helicase Ddx39b OS=Mus musculus OX=10090 GN=Ddx39b PE=1 SV=1 | 41,52 | 138,49 |
| Q9DBR7 | Protein phosphatase 1 regulatory subunit 12A OS=Mus musculus OX=10090 GN=Ppp1r12a PE=1 SV | 40,32 | 223,47 |
| P43247 | DNA mismatch repair protein Msh2 OS=Mus musculus OX=10090 GN=Msh2 PE=1 SV=1 | 39,19 | 5,66 |
| Q8C4Y3 | Negative elongation factor B OS=Mus musculus OX=10090 GN=Nelfb PE=1 SV=2 | 38,35 | 56,50 |
| Q3U2K0 | Protein FAM193B OS=Mus musculus OX=10090 GN=Fam193b PE=1 SV=2 | 37,69 | 114,22 |
| Q9JLC8 | Sacsin OS=Mus musculus OX=10090 GN=Sacs PE=1 SV=2 | 37,66 | 16,76 |
| Q9DBD5 | Proline-, glutamic acid- and leucine-rich protein 1 OS=Mus musculus OX=10090 GN=Pelp1 PE=1 SV= | 37,61 | 265,18 |
| Q640N1 | Adipocyte enhancer-binding protein 1 OS=Mus musculus OX=10090 GN=Aebp1 PE=1 SV=1 | 36,99 | 31,31 |
| P01942 | Hemoglobin subunit alpha OS=Mus musculus OX=10090 GN=Hba PE=1 SV=2 | 34,96 | 11,52 |
| Q62159 | Rho-related GTP-binding protein RhoC OS=Mus musculus OX=10090 GN=Rhoc PE=1 SV=2 | 34,69 | 185,17 |
| P47757 | F-actin-capping protein subunit beta OS=Mus musculus OX=10090 GN=Capzb PE=1 SV=3 | 32,48 | 16,89 |
| Q91V81 | RNA-binding protein 42 OS=Mus musculus OX=10090 GN=Rbm42 PE=1 SV=1 | 32,34 | 15,45 |
| Q91VZ6 | Stromal membrane-associated protein 1 OS=Mus musculus OX=10090 GN=Smap1 PE=1 SV=1 | 31,60 | 18,60 |
| P08207 | Protein S100-A10 OS=Mus musculus OX=10090 GN=S100a10 PE=1 SV=2 | 30,54 | 8,42 |
| P39447 | Tight junction protein ZO-1 OS=Mus musculus OX=10090 GN=Tjp1 PE=1 SV=2 | 30,47 | 11,64 |
| P50518 | V-type proton ATPase subunit E 1 OS=Mus musculus OX=10090 GN=Atp6v1e1 PE=1 SV=2 | 30,37 | 25,75 |
| Q8CGY8 | UDP-N-acetylglucosamine--peptide N-acetylglucosaminyltransferase 110 kDa subunit OS=Mus mus | 28,22 | 85,37 |
| P47753 | F-actin-capping protein subunit alpha-1 OS=Mus musculus OX=10090 GN=Capza1 PE=1 SV=4 | 27,33 | 106,23 |
| Q810A7 | ATP-dependent RNA helicase DDX42 OS=Mus musculus OX=10090 GN=Ddx42 PE=1 SV=3 | 26,06 | 5,02 |
| P97384 | Annexin A11 OS=Mus musculus OX=10090 GN=Anxa11 PE=1 SV=2 | 25,55 | 14,79 |
| P33215 | Protein NEDD1 OS=Mus musculus OX=10090 GN=Nedd1 PE=1 SV=2 | 24,87 | 10,94 |
| Q9CWN7 | CCR4-NOT transcription complex subunit 11 OS=Mus musculus OX=10090 GN=Cnot11 PE=1 SV=1 | 24,83 | 26,80 |
| P02088 | Hemoglobin subunit beta-1 OS=Mus musculus OX=10090 GN=Hbb-b1 PE=1 SV=2 | 24,58 | 31,89 |
| Q80XI3 | Eukaryotic translation initiation factor 4 gamma 3 OS=Mus musculus OX=10090 GN=Eif4g3 PE=1 SV | 23,33 | 17,29 |
| P02104 | Hemoglobin subunit epsilon-Y2 OS=Mus musculus OX=10090 GN=Hbb-y PE=1 SV=2 | 22,68 | 25,66 |
| P62141 | Serine/threonine-protein phosphatase PP1-beta catalytic subunit OS=Mus musculus OX=10090 GN | 21,59 | 11,16 |
| P70218 | Mitogen-activated protein kinase kinase kinase kinase 1 OS=Mus musculus OX=10090 GN=Map4k1 | 21,55 | 23,87 |
| Q3UMT1 | Protein phosphatase 1 regulatory subunit 12C OS=Mus musculus OX=10090 GN=Ppp1r12c PE=1 SV | 21,51 | 18,11 |
| Q80YR4 | E3 ubiquitin-protein ligase ZNF598 OS=Mus musculus OX=10090 GN=Znf598 PE=1 SV=1 | 21,19 | 18,22 |
| Q91YR7 | Pre-mRNA-processing factor 6 OS=Mus musculus OX=10090 GN=Prpf6 PE=1 SV=1 | 20,40 | 9,91 |
| P08113 | Endoplasmin OS=Mus musculus OX=10090 GN=Hsp90b1 PE=1 SV=2 | 20,17 | 15,06 |
| Q6PCZ4 | Melanoma-associated antigen E1 OS=Mus musculus OX=10090 GN=Magee1 PE=1 SV=1 | 19,06 | 117,44 |
| P19426 | Negative elongation factor E OS=Mus musculus OX=10090 GN=Nelfe PE=1 SV=2 | 18,86 | 308,39 |
| Q91VR8 | Protein BRICK1 OS=Mus musculus OX=10090 GN=Brk1 PE=1 SV=1 | 18,86 | 28,99 |
| P98064 | Mannan-binding lectin serine protease 1 OS=Mus musculus OX=10090 GN=Masp1 PE=1 SV=2 | 18,38 | 32,32 |
| P68181 | cAMP-dependent protein kinase catalytic subunit beta OS=Mus musculus OX=10090 GN=Prkacb PE | 18,25 | 18,04 |
| Q8BZN4 | NUAK family SNF1-like kinase 2 OS=Mus musculus OX=10090 GN=Nuak2 PE=1 SV=2 | 18,00 | 80,23 |
| Q9D554 | Splicing factor 3A subunit 3 OS=Mus musculus OX=10090 GN=Sf3a3 PE=1 SV=2 | 16,83 | 29,10 |
| P47754 | F-actin-capping protein subunit alpha-2 OS=Mus musculus OX=10090 GN=Capza2 PE=1 SV=3 | 16,22 | 82,93 |
| Q02384 | Son of sevenless homolog 2 OS=Mus musculus OX=10090 GN=Sos2 PE=1 SV=2 | 15,17 | 12,15 |
| E9QAM5 | Helicase with zinc finger domain 2 OS=Mus musculus OX=10090 GN=Helz2 PE=1 SV=1 | 14,54 | 7,01 |
| A2AF47 | Dedicator of cytokinesis protein 11 OS=Mus musculus OX=10090 GN=Dock11 PE=1 SV=1 | 14,04 | 83,58 |
| P58021 | Transmembrane 9 superfamily member 2 OS=Mus musculus OX=10090 GN=Tm9sf2 PE=1 SV=1 | 13,72 | 72,64 |
| Q3TZX8 | Polynucleotide 5'-hydroxyl-kinase NOL9 OS=Mus musculus OX=10090 GN=Nol9 PE=1 SV=1 | 13,70 | 33,27 |
| O70274 | Protein tyrosine phosphatase type IVA 2 OS=Mus musculus OX=10090 GN=Ptp4a2 PE=1 SV=1 | 13,68 | 8,96 |
| Q61136 | Serine/threonine-protein kinase PRP4 homolog OS=Mus musculus OX=10090 GN=Prpf4b PE=1 SV= | 13,41 | 13,16 |
| Q9CY57 | Chromatin target of PRMT1 protein OS=Mus musculus OX=10090 GN=Chtop PE=1 SV=2 | 13,14 | 31,22 |
| Q9ZZK1 | Keratin, type I cytoskeletal 16 OS=Mus musculus OX=10090 GN=Krt16 PE=1 SV=3 | 12,90 | 6,01 |
| Q9JJ80 | Ribosome production factor 2 homolog OS=Mus musculus OX=10090 GN=Rpf2 PE=2 SV=2 | 12,68 | 8,70 |
| Q61990 | Poly(rC)-binding protein 2 OS=Mus musculus OX=10090 GN=Pcbp2 PE=1 SV=1 | 12,52 | 9,16 |
| Q91WN1 | Dnal homolog subfamily C member 9 OS=Mus musculus OX=10090 GN=Dnajc9 PE=1 SV=2 | 12,35 | 6,53 |
| Q921Q7 | Ras and Rab interactor 1 OS=Mus musculus OX=10090 GN=Rin1 PE=1 SV=1 | 12,29 | 12,55 |
| Q9Z315 | U4/U6.U5 tri-snRNP-associated protein 1 OS=Mus musculus OX=10090 GN=Sart1 PE=1 SV=1 | 11,10 | 7,03 |
| Q62203 | Splicing factor 3A subunit 2 OS=Mus musculus OX=10090 GN=Sf3a2 PE=1 SV=2 | 11,10 | 10,83 |
| Q8BG30 | Negative elongation factor A OS=Mus musculus OX=10090 GN=Nelfa PE=1 SV=1 | 11,02 | 10,01 |
| Q60930 | Voltage-dependent anion-selective channel protein 2 OS=Mus musculus OX=10090 GN=Vdac2 PE= | 10,90 | 5,91 |
| Q8K1N4 | Spermatogenesis-associated serine-rich protein 2 OS=Mus musculus OX=10090 GN=Spats2 PE=1 SV | 10,87 | 9,51 |
| P97434 | Myosin phosphatase Rho-interacting protein OS=Mus musculus OX=10090 GN=Mprip PE=1 SV=2 | 10,45 | 16,65 |
| Q9CY27 | Very-long-chain enoyl-CoA reductase OS=Mus musculus OX=10090 GN=Tecr PE=1 SV=1 | 9,99 | 8,68 |
| E9Q1P8 | Interferon regulatory factor 2-binding protein 2 OS=Mus musculus OX=10090 GN=Irf2bp2 PE=1 SV= | 9,99 | 31,05 |
| Q6Y685 | Transforming acidic coiled-coil-containing protein 1 OS=Mus musculus OX=10090 GN=Tacc1 PE=1 S | 9,97 | 24,61 |
| Q921M3 | Splicing factor 3B subunit 3 OS=Mus musculus OX=10090 GN=Sf3b3 PE=1 SV=1 | 9,84 | 5,69 |
| A2AMM0 | Caveolae-associated protein 4 OS=Mus musculus OX=10090 GN=Cavin4 PE=1 SV=1 | 9,82 | 16,96 |
| Q02819 | Nucleobindin-1 OS=Mus musculus OX=10090 GN=Nucb1 PE=1 SV=2 | 9,65 | 74,93 |
| Q0P678 | Zinc finger CCCH domain-containing protein 18 OS=Mus musculus OX=10090 GN=Zc3h18 PE=1 SV= | 9,43 | 9,72 |
| Q9EP71 | Ankycorbin OS=Mus musculus OX=10090 GN=Rai14 PE=1 SV=1 | 9,08 | 17,43 |
| P29391 | Ferritin light chain 1 OS=Mus musculus OX=10090 GN=Ftl1 PE=1 SV=2 | 8,99 | 11,83 |
| Q62556 | Butyrophilin subfamily 1 member A1 OS=Mus musculus OX=10090 GN=Btn1a1 PE=1 SV=2 | 8,91 | 100,55 |
| Q6ZQ08 | CCR4-NOT transcription complex subunit 1 OS=Mus musculus OX=10090 GN=Cnot1 PE=1 SV=2 | 8,91 | 10,81 |
| Q80TY0 | Formin-binding protein 1 OS=Mus musculus OX=10090 GN=Fnbp1 PE=1 SV=2 | 8,76 | 9,32 |
| O54988 | STE20-like serine/threonine-protein kinase OS=Mus musculus OX=10090 GN=Slk PE=1 SV=2 | 7,98 | 18,48 |
| Q9CW03 | Structural maintenance of chromosomes protein 3 OS=Mus musculus OX=10090 GN=Smc3 PE=1 SV | 7,98 | 8,27 |
| Q923Z0 | G-protein coupled receptor family C group 5 member B OS=Mus musculus OX=10090 GN=Gprc5b P | 7,92 | 359,79 |
| Q9WV55 | Vesicle-associated membrane protein-associated protein A OS=Mus musculus OX=10090 GN=Vapa | 7,92 | 7,23 |
| Q149F3 | Eukaryotic peptide chain release factor GTP-binding subunit ERF3B OS=Mus musculus OX=10090 G | 7,91 | 24,52 |
| Q922L6 | Negative elongation factor D OS=Mus musculus OX=10090 GN=Nelfcd PE=1 SV=2 | 7,88 | 42,41 |
| Q8BFX3 | BTB/POZ domain-containing protein KCTD3 OS=Mus musculus OX=10090 GN=Kctd3 PE=1 SV=1 | 7,61 | 11,43 |
| P07356 | Annexin A2 OS=Mus musculus OX=10090 GN=Anxa2 PE=1 SV=2 | 7,49 | 5,42 |
| Q9ES28 | Rho guanine nucleotide exchange factor 7 OS=Mus musculus OX=10090 GN=Arhgef7 PE=1 SV=2 | 7,43 | 22,92 |
| P29788 | Vitronectin OS=Mus musculus OX=10090 GN=Vtn PE=1 SV=2 | 7,35 | 22,23 |
| Q9JKY0 | CCR4-NOT transcription complex subunit 9 OS=Mus musculus OX=10090 GN=Cnot9 PE=1 SV=1 | 6,82 | 64,85 |
| Q8C5L3 | CCR4-NOT transcription complex subunit 2 OS=Mus musculus OX=10090 GN=Cnot2 PE=1 SV=2 | 6,77 | 19,82 |
| Q9CQQ4 | Gem-associated protein 2 OS=Mus musculus OX=10090 GN=Gemin2 PE=2 SV=1 | 6,40 | 18,74 |
| P28660 | Nck-associated protein 1 OS=Mus musculus OX=10090 GN=Nckap1 PE=1 SV=2 | 6,06 | 6,65 |
| Q60596 | DNA repair protein XRCC1 OS=Mus musculus OX=10090 GN=Xrcc1 PE=1 SV=2 | 5,84 | 8,38 |
| Q3TKT4 | Transcription activator BRG1 OS=Mus musculus OX=10090 GN=Smarca4 PE=1 SV=1 | 5,69 | 6,69 |
| Q8R0X7 | Sphingosine-1-phosphate lyase 1 OS=Mus musculus OX=10090 GN=Sgpl1 PE=1 SV=1 | 5,54 | 9,17 |
| Q8VED5 | Keratin, type II cytoskeletal 79 OS=Mus musculus OX=10090 GN=Krt79 PE=1 SV=2 | 5,52 | 5,93 |
| P84084 | ADP-ribosylation factor 5 OS=Mus musculus OX=10090 GN=Arf5 PE=1 SV=2 | 5,38 | 6,45 |
| Q8D5W1 | S-adenosylhomocysteine hydrolase-like protein 1 OS=Mus musculus OX=10090 GN=Ahcyl1 PE=1 SV | 5,27 | 5,73 |

Supplementary Table 3

341 **Table S4. Primers for site-direct mutagenesis.**

| Primer Name | Oligonucleotide sequence (5'-3') |
|---|---|
| MuRF2 C42S His/Myc for | GCCTGTGGTCATTCTCCCTAGCCAGCACAA |
| MuRF2 C42S His/Myc rev | TTCGTGAACATCTCTAGGCAGATGGGACAG |
| MuRF2 C50S His/Myc for | GCACAACCTGTGCAGGAAAAGTGCCAGTGACATC |
| MuRF2 C50S His/Myc rev | TGGCAAGGGAGAATGACCACAGGCTTCGTGAACA |
| MuRF3 C42S His/Myc for | CCCGTGGTGATCTTGCCCAGCCAACACAAC |
| MuRF3 C42S His/Myc rev | CTTGGAGAACATCTCCAGGCAGATGG |
| MuRF3 C50S His/Myc for | CTGTGCCGCAAGAGTGCCAACGACGTCTTC |
| MuRF3 C50S His/Myc rev | GTTGTGTTGGCAGGGCAAGATCACCACGGG |
| SNX5 K290R for | GTCTCATCAGATGAAGACTTAAGACTGACAGAGCT CCTCCGATAC |
| SNX5 K290R rev | GTATCGGAGGAGCTCTGTCAGTCTTAAGTCTTCATC TGATGAGAC |
| SNX5 K324R for | GACTATGAGAATTCAAACAGAGCTTTGGACAAGGC CCGG |
| SNX5 K324R rev | CCGGGCCTTGTCCAAAGCTCTGTTTGAATTCTCATA GTC |

342

343 **Table S5. Primers for generation of retroviral expression plasmid.**

| Primer Name | Oligonucleotide sequence (5'-3') |
|---|---|
| SNX5 His/Myc for (NotI) | ATAAGAATGCGGCCGCATTCTTATGGCCGCGGTTC |
| SNX5 His/Myc rev (NotI) | ATAGTTTAGCGGCCGCTCAATGATGATGATGATGATG |

344

345 **Table S6. Primers for quantitative real-time PCR.**

| Primer Name | Oligonucleotide sequence (5'-3') |
|---|---|
| Mm_Snx5 for | GTTCCCGAGTTGCTGGAG |
| Mm_Snx5 rev | GCGATGGGTCAACATTCAG |
| Mm_Prkar1a for | TGATGCTATGTTTCCAGTCTCC |
| Mm_Prkar1a rev | CAATCACATAGAAGTTATCCCCTTC |
| Mm_Mymk for | ATCGCTACCAAGAGGCGTT |
| Mm_Mymk rev | CACAGCACAGACAAACCAGG |
| Mm_Mymx for | CAGGAGGGCAAGAAGTTCAG |
| Mm_Mymx rev | ATGTCTTGGGAGCTCAGTCG |
| Mm_Myog for | GACTTGACCTTGGACCTTGG |
| Mm_Myog rev | CGCTGTGGGAGTTGCATT |
| Mm_Ache for | GGGCTCCTACTTTCTGGTTTAC |
| Mm_Ache rev | TTCAGGTTCAGGCTCACATATT |
| Mm_Hdac5 for | GCATGAACTCTCCCAACGAG |
| Mm_Hdac5 rev | TTCACCTCCACTGCCACAG |
| Mm_Myh1 for | GAAGATGTTCCTGTGGATGG |
| Mm_Myh1 rev | TCGTTGGTGAAGTTGATGC |
| Mm_Myh2 for | AACTCCAGGCAAAAGTGAAATC |
| Mm_Myh2 rev | TGGATAGATTTGTGTTGGATTGTT |
| Mm_Myh3 for | AGTAGCCAGGATGGGAAAGTC |
| Mm_Myh3 rev | GTCCTCTGGCTTAACCACCA |
| Mm_Myh4 for | GGGAACATGAAATTCAAGCAA |
| Mm_Myh4 rev | ATAGGCAGCCTTGTCAGCAA |
| Mm_Myh7 for | CGCATCAAGGAGCTCACC |

| | |
|---|---|
| Mm_Myh7 rev | CTGCAGCCGCAGTAGGTT |
| Mm_Mstn for | AGGGCAGTGAGAGAGAAGAA |
| Mm_Mstn rev | GTTTCCGTGGTAGCGTGATAA |
| Mm_Mstn-promoter for | ACAGCACTCCAAGTCTTAAAGG |
| Mm_Mstn- promoter rev | TCACAAGTCACCAAGCAGTATT |
| Mm_RPL30 for | TGGTGTTTGACGCTCTGG |
| Mm_RPL30 rev | GTTGGAGCCTAGAGTTGATCG |
| Mm_Gapdh for | GATCAAACGCTTGCGAATCT |
| Mm_Gapdh rev | ATGGTGAAGGTCGGTGTGA |

346

**Table S7. nano-LC MS/MS and search parameters**

*A. Description of the LC-MS/MS experiment settings – Ultimate-QExactive Plus configuration*

| **nanoLC-parameters for the chromatographic separation of the peptides** | |
|---|---|
| Equipment | Ultimate 3000 (Thermo Electron, Bremen, Germany) |
| Trap column | Acclaim PepMap 100-C18 trap column (2cm x75µm, 3µm, 100Å) Thermo Fisher Scientific Inc., Idstein, Germany |
| Analytical column | Accucore 150-C18 column (25cm x 2.6µm, 2.6µm, 150Å) Thermo Fisher Scientific Inc., Idstein, Germany |
| Buffer system | 0.1% acetic acid, 5% ACN in water (buffer A) and 100% ACN in 0.1% acetic acid (buffer B) |
| Flow rate | 300nL/min |
| Gradient | linear gradient of buffer B from 5% up to 25% for 120 min |
| Column oven temperature | 40°C |
| **Mass Spectrometry** | |
| Equipment | QExactive Plus |
| Ion source | FlexMap Ion source (Thermo Scientific) |
| Fragmentation | high-energy collision dissociation (HCD) |
| Charge state screening | positive |

| DDA acquisition | |
|---|---|
| **Full MS** | |
| MS scan resolution | 70,000 |
| AGC target | 3 x 10E6 |
| Maximum ion injection time for the MS scan | 120 ms |
| MS full scan range | 300 to 1650 m/z |
| Spectra data type | profile |
| **dd-MS2** | |
| Resolution | 17,500 |
| AGC target | 2 x 10E5 |
| Maximum ion injection time for the MS2 scan | 120 ms |
| Selection | Top10 z= +2 to +6 charge state |
| Isolation width | 3.0 m/z |
| Scan range | 200 to 2,000 m/z |
| Fixed first mass | 100 m/z |
| Spectrum data type | centroid |
| Minimum AGC target | 1 x 10E4 |
| Intensity threshold | 8.3 x 10E4 |
| Monoisotopic precursor selection rejected | +1 and +7, +8, and >+8 charged ions |
| Dynamic exclusion | 30 s |
| Normalized collision energy | 27.5eV |

350

351 *B. Presentation of Protein Identification Results*

| **Protein identification/quantitation** |
|---|

| **Search parameters** | **Settings** |
|---|---|
| Name of peaklist-generating software and release version (number or date) | Proteome discoverer 2.3 (Thermo Scientific) using SequestHT as search engine |
| Protein database | Uniprot/Swissprot database limited to murine entries (version 11_2019) |
| Enzyme specificity considered | Fully tryptic |
| Precursor mass tolerance | 10 ppm |
| Fragment mass tolerance | 0.02 Da |
| # of missed cleavages permitted | 2 |
| Static modification | carbamidomethylation at cysteine |
| Variable modification | oxidation at methionine; acetylation at protein N-terminus |
| FDR (peptide level) | 1% |
| Data quantification | MS1 peak area of precursor |

352

353 **Supplementary Figures**

354 **Figure S1. A SILAC-AP-MS approach identified the novel MuRF3 interaction partner**
355 **SNX5.** (A) Workflow of the SILAC-AP-MS approach. (B) Western blot analysis of proteins
356 isolated from different murine organs as indicated. (C) qRT-PCR analysis of *Snx5* in different
357 murine organs as indicated. *Snx5* mRNA expression was normalized to *Gapdh*.

358 **Figure S2. MuRF3 reduces MuRF2-dependent SNX5 degradation.** (A) C2C12 cells were
359 cotransfected with increasing amounts of MuRF2-[(C42S;C50S)]-Myc(His)6, and a constant
360 amount of SNX5-FLAG. Cells were lysed 24 h later and overexpressed proteins were analyzed
361 by Western blot using anti-Myc and anti-FLAG antibodies. (B) Western blot analysis of C2C12
362 cells co-transfected with SNX5-FLAG, MuRF2- or increasing amounts of MuRF3-Myc$(His)_6$
363 as indicated.

364 **Figure S3. MuRF2-mediated reduction in SNX5 stability is mediated by its K290 and**
365 **K324.** (A) PyMOL visualization of putative ubiquitin chain binding sites on SNX5 (PDB
366 5tp1D) at K290 and K324 (indicated in red). (B) Schematic showing SNX5 ubiquitination sites
367 and K290R, K324R, K290/324R mutants. (C) Cycloheximide (CHX) chase assay in COS7
368 cells. MuRF2-Myc$(His)_6$ was co-transfected with either SNX5-FLAG or each of K290R,
369 K324R, K290/324R mutants for 48 hours. Cells were then treated with CHX for indicated time
370 points prior to lysis. Proteins were analyzed by Western blot using the indicated antibodies.

371 **Figure S4. SNX5 stabilizes RI-α upon PKA activation.** (A) Workflow for identification of
372 SNX5 cargo proteins via mass spectrometry. (B) Sucrose gradient fractionation of PNS isolated
373 from C2C12 cells followed by Western blotting with the indicated antibodies. Individual
374 fractions are indicated. (C) DSS cross-linking of core RI-α oligomers detected via Western blot
375 in vehicle- or Bt2cAMP-treated C2C12 cells. Densitometrical analysis (right panel) was carried
376 out in Image Lab$^{TM}$ software. PKA tetramer-to-RI-α ratios are shown. (D) Immunofluorescence
377 using anti-RI-α (green) and anti-EEA1 (red) antibody in vehicle- or Bt2cAMP and CHX treated
378 NT-WT and SNX5-KO C2C12 myoblasts for 1 or 4 hours. Nuclei were stained with DAPI.

Scale bar, 20 μm. (E) Workflow to enrich endosomal fractions from SNX5-KO and NT-WT myocytes. (F) Work flow of protease protection assay. (G) PNGase F digestion assay, SNX5-coated endosomes isolated from C2C12 cells by IP SNX5 were digested with PNGase F. Western blot with anti-RI-α antibody was performed.

**Figure S5. PKA activation is accompanied by an increase in *Prkar1a* expression in SNX5-KO myocytes.** qRT-PCR analysis of *Prkar1a* expression in NT-WT and SNX5-KO cells treated with either vehicle or Bt2cAMP for the indicated time points. *Prkar1a* mRNA expression was normalized to *Gapdh*. Statistical significance was determined using one-way ANOVA followed by Tukey's post-hoc test. *$P < 0.05$, **$P < 0.01$, ***$P < 0.001$, ****$P < 0.0001$.

**Figure S6. Reintroduction of SNX5 in SNX5-KO myocytes increases the stability of RI-α.** Western blot analysis of eGFP or SNX5-Myc(His)$_6$ transduced SNX5-KO myoblasts treated with Bt2cAMP and CHX for indicated time points prior to cell lysis. Densitometric analysis of RI-α levels was carried out in Image Lab™ Software, with the "0-hour" intensity of RI-α set as 1. Protein amounts of RI-α were normalized to GAPDH and RI-α-to-GAPDH ratios per indicated time point are shown.

**Figure S7. SNX5 stabilizes RI-α upon PKA activation.** (A, B) Western blot of NT-siRNA or SNX5-siRNA transfected C2C12 myoblasts (A) and myotubes (B) co-treated with Bt2cAMP, CHX, and the inhibitors as indicated for 4 hours.

**Figure S8. Reduction in free RI-α upon PKA activation is mediated by proteasomal protein degradation in SNX5-HET cells.** Western blot analysis of NT-WT and SNX5-HET C2C12 myoblasts treated with Bt2cAMP, CHX, and one of the indicated inhibitors (MG132, CQ, or BafA1) for 4 hours prior to cell lysis.

**Figure S9. SNX5 via regulation of PKA activity contributes to myogenic differentiation.** (A) qRT-PCR analysis of *Hdac5* mRNA expression from C2C12 cells treated with Bt2cAMP for different time points. *Hdac5* mRNA expression was normalized to *Gapdh*. Data were

analyzed with one-way ANOVA followed by Tukey's post-hoc test. ****P < 0.0001. (B) Nuclear and cytoplasmic fractionation followed by Western blot analysis of NT-WT and SNX5-KO C2C12 cells with indicated antibodies. (C) Western blot analysis of vehicle or recombinant myostatin treated C2C12 myotubes (MT3) for 3 days.

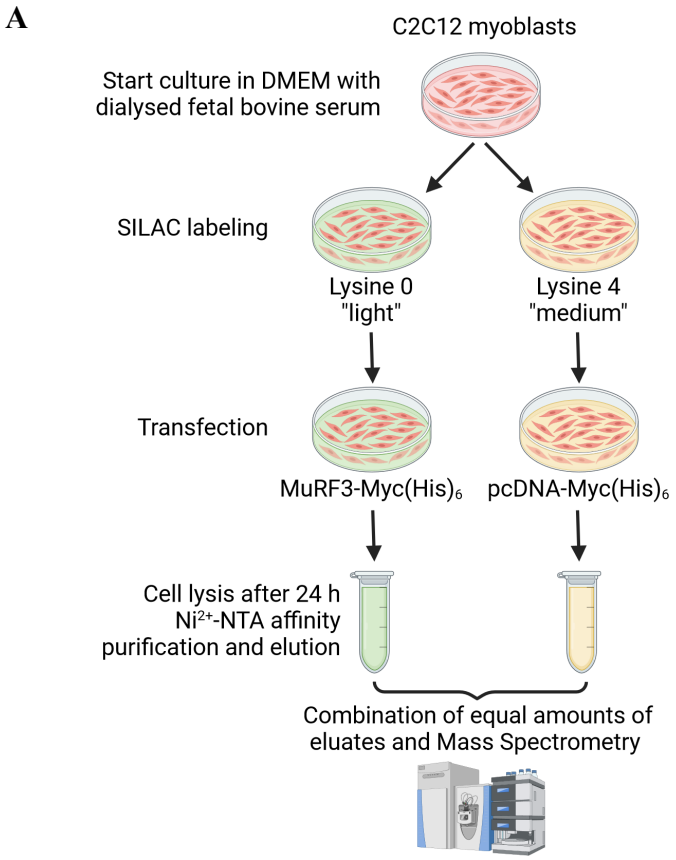


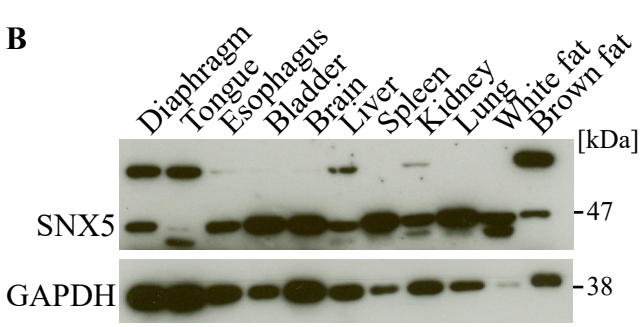


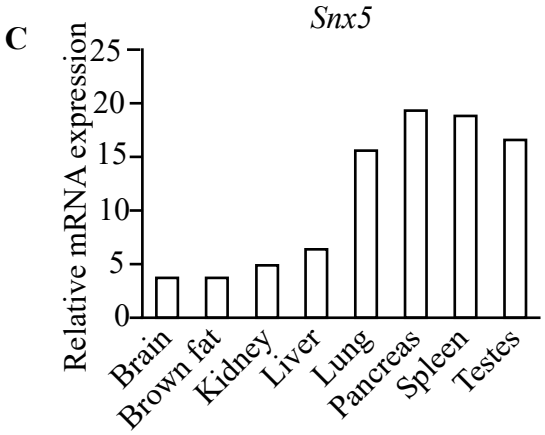


Supplementary Figure 1

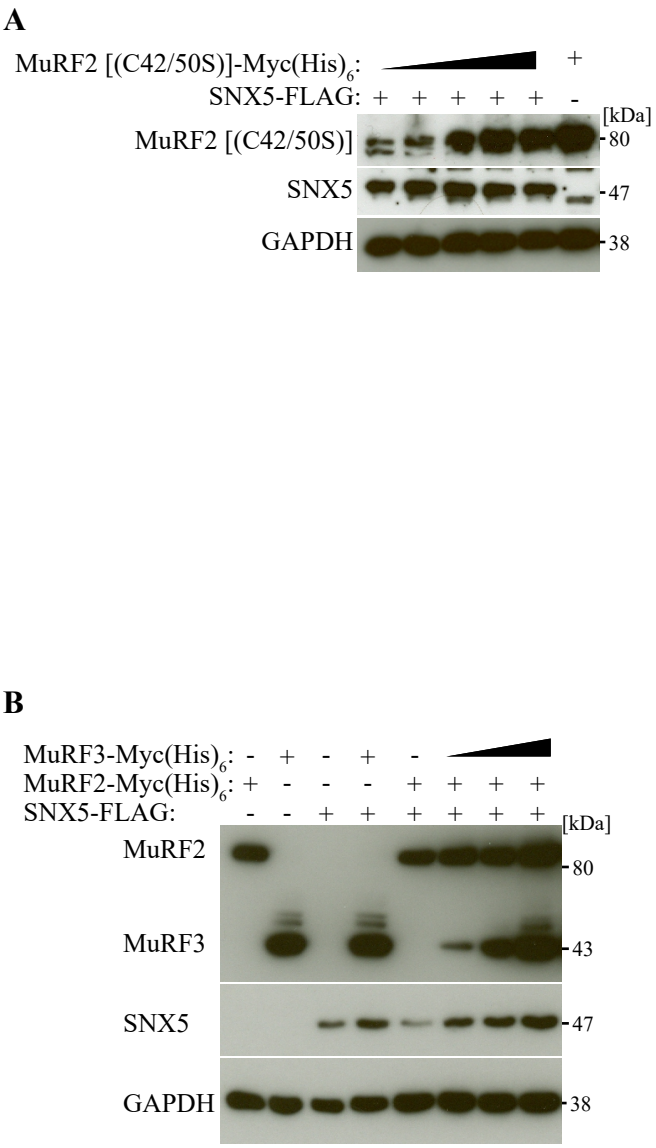


Supplementary Figure 2

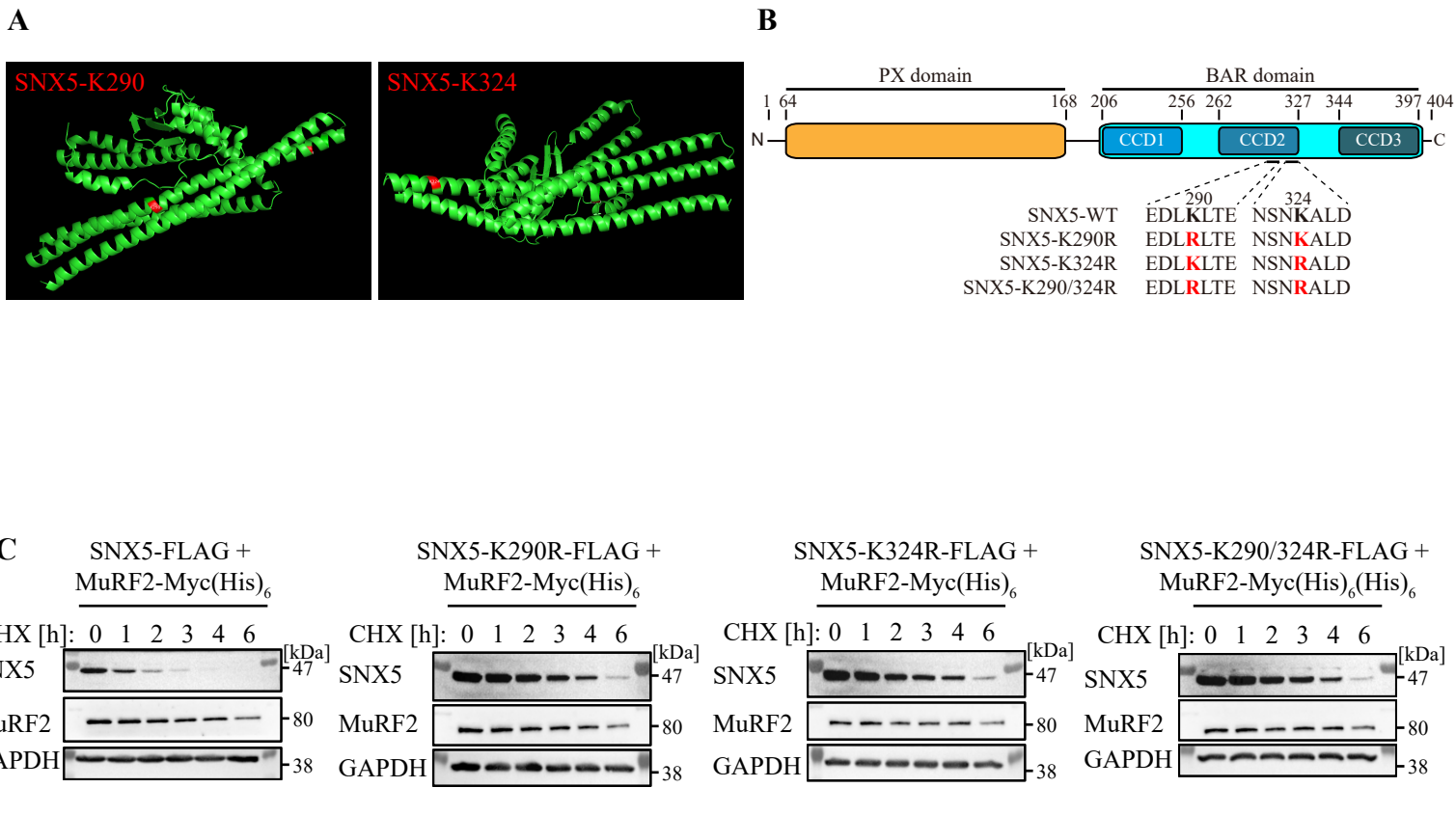


Supplementary Figure 3

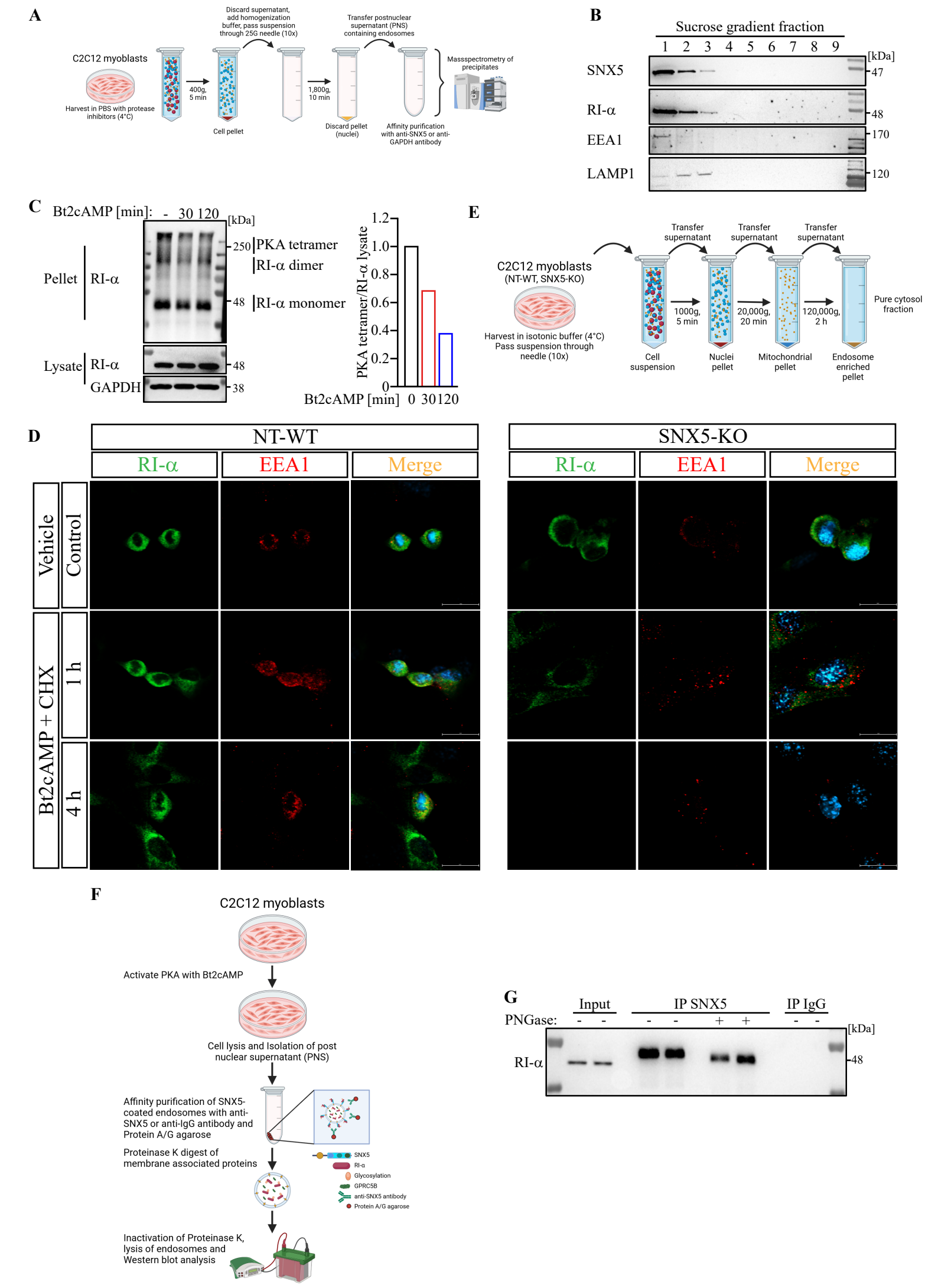


Supplementary Figure 4

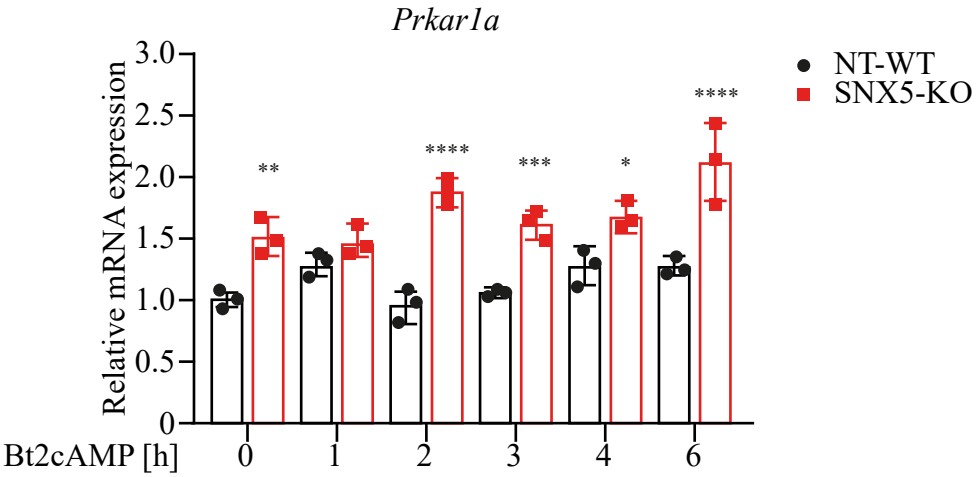


Supplementary Figure 5

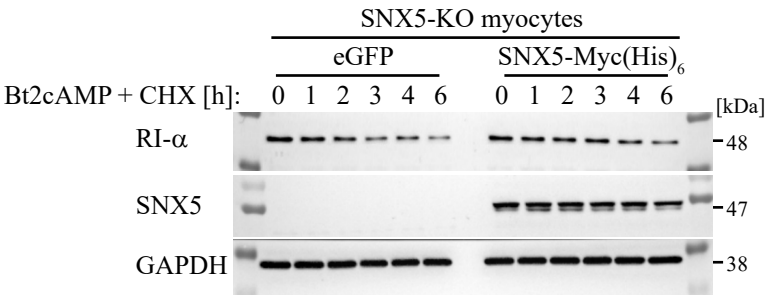


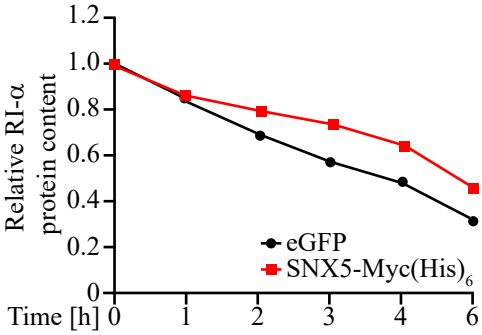


Supplementary Figure 6

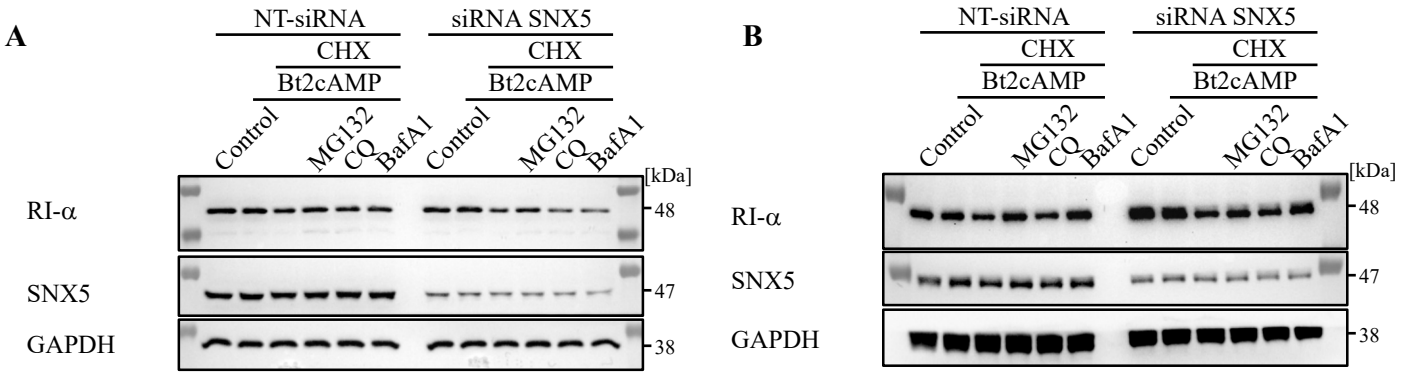


Supplementary Figure 7

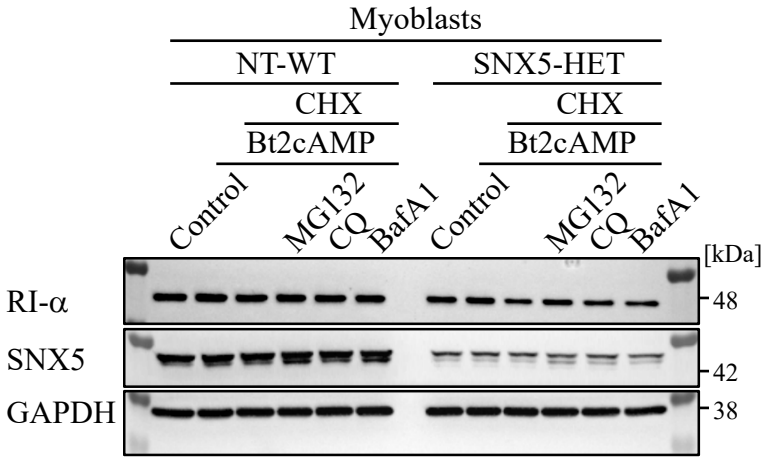


Supplementary Figure 8

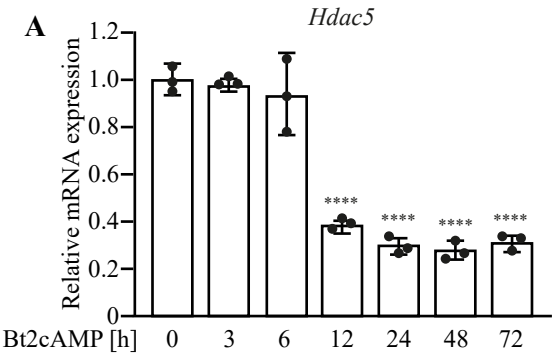


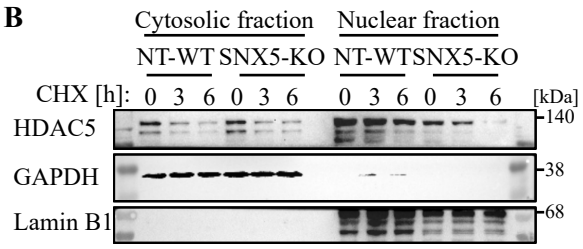


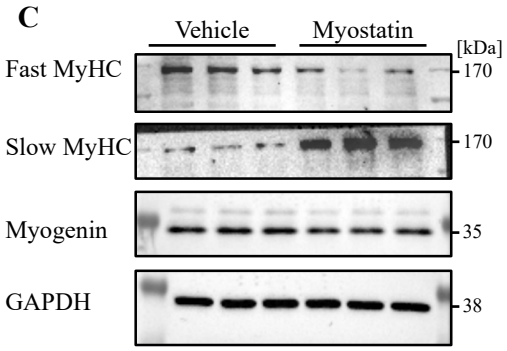


Supplementary Figure 9